Pathology & Oncology Research (2019) 25:1199–1206
https://doi.org/10.1007/s12253-019-00601-8

ORIGINAL ARTICLE

Correlations between Histological and Array Comparative Genomic Hybridization Characterizations of Wilms Tumor

Ming-Ru Chiang[1] · Chi-Wen Kuo[2,3,4,5] · Wen-Chung Wang[6] · Tai-Cheng Hou[7] · Chen-Yun Kuo[7] · Meng-Yao Lu[8] · Yen-Chein Lai[9]

Received: 29 October 2018 / Accepted: 15 January 2019 / Published online: 23 January 2019

Abstract

Wilms tumor, or nephroblastoma, is the most common pediatric renal malignancy. Its diagnosis is principally based on histology. Several genetic loci have been shown to be associated with Wilms tumor formation, including *WT1*, *WT2*, *FWT1*, *FWT2, CTNNB1*, *WTX*, and *TP53*. Other loci, such as 1p, 2q, 7p, 9q, 12q, 14q, 16q, 17p, and 22, have also been implicated in the etiology of Wilms tumor. The aim of this study is to elucidate the molecular pathogenesis of this tumor. In the present study, we analyzed the histological appearance and copy number aberrations using array comparative genomic hybridization of six Wilms tumors without somatic mutation in the *WT1* gene. Many chromosomal aberrations on array comparative genomic hybridization analysis revealed that the genetics of Wilms tumors are extremely complex. Amplifications and deletions of large DNA fragments were observed in some samples. Amplifications of *NDUFV1*, *ZIC2*, *SIX1*, *NR2F2, MIR1469*, *SOX9*, *JAG1*, *MIR6870,* and *GNAS* were found in all six Wilms tumors. Moreover, amplifications of five genes were identified in the Wilms tumors of stromal type and amplifications of at least 10 genes were identified in the Wilms tumors of epithelial type. Our results indicated that amplifications of nine genes are the essential events in the tumorigenesis of Wilms tumor, which may inform its clinical and therapeutic management. In addition, mixed type Wilms tumor may be the heterogeneous group able to be classified using genetic results of epithelial and stromal components based on immunohistochemistry.

Keywords Wilms tumor · Nephroblastoma · Array comparative genomic hybridization · Molecular pathogenesis

Introduction

Wilms tumor, or nephroblastoma, is an embryonal tumor of the kidney and the most frequently occurring solid tumor of childhood, excluding brain tumors [1–3]. In the Caucasian population, age-standardized annual incidence rates of 6 to 9 per million have been reported for Wilms tumor [4]. In Taiwan, the average annual incidence rate is 2.9 per million children under 15 years of age [5]. Data obtained from the Childhood Cancer Foundation in Taiwan indicate that 7 to

Electronic supplementary material The online version of this article (https://doi.org/10.1007/s12253-019-00601-8) contains supplementary material, which is available to authorized users.

✉ Yen-Chein Lai
yenchein@csmu.edu.tw

[1] Department of Pediatrics, Jen-Ai Hospital, 483 Dong Rong Road, Taichung 412, Taiwan

[2] Department of Pharmacy, Jen-Ai Hospital, 483 Dong Rong Road, Taichung 412, Taiwan

[3] School of Pharmacy, College of Pharmacy, China Medical University, 91 Hsueh-Shih Road, Taichung 404, Taiwan

[4] Basic Medical Education Center, Central Taiwan University of Science and Technology, 666 Buzih Road, Taichung 406, Taiwan

[5] Department of Health Policy and Management, Chung Shan Medical University, 110 Sec 1, Chien Kuo N Road, Taichung 402, Taiwan

[6] Department of Obstetrics and Gynecology, Jen-Ai Hospital, 483 Dong Rong Road, Taichung 412, Taiwan

[7] Department of Pathology, Jen-Ai Hospital, 483 Dong Rong Road, Taichung 412, Taiwan

[8] Department of Pediatrics, National Taiwan University Hospital, 8 Chung-Shan South Road, Taipei 100, Taiwan

[9] Department of Medical Laboratory and Biotechnology, Chung Shan Medical University, No.110, Sec 1, Chien Kuo North Road, Taichung 402, Taiwan

18 new cases of Wilms tumor are diagnosed each year (1992 to 2000) [5].

Several genes and chromosomal areas have been shown to be associated with tumor formation, including *WT1* at chromosome 11p13, *WT2* at 11p15, *FWT1* (*WT4*) at 17q12–21, and *FWT2* at 19q13.33–13.41 [6, 7]. More recently, *CTNNB1* at 3p22.1, *WTX* at Xq11.1, and *TP53* at 17p13 have been added to this list [8]. *WT1* was the first and most important gene to be isolated [9]. Other loci, including 1p, 2q, 7p, 9q, 12q, 14q, 16q, 17p, and 22, have also been implicated in the etiology of Wilms tumor [10, 11]. The risk of Wilms tumor conferred by mutations and epigenetic changes associated with these loci has been poorly characterized in Taiwan. From our previous studies, most DNA samples from peripheral blood lymphocytes and paraffin-embedded tumor specimens of Wilms tumors test negative for both constitutional mutations and somatic mutations in the *WT1* gene [12].

Over the past decade, few array comparative genomic hybridization (aCGH) analyses of Wilms tumors using human whole-genome bacterial artificial chromosome (BAC) microarrays at 1-Mb resolution have been conducted [13, 14]. With the advent of oligonucleotide arrays for CGH analysis, higher resolution mapping of DNA copy number changes has become available for clinical samples [15]. The aim of the present study is to analyze the histological appearance and copy number aberrations using aCGH technology of six Wilms tumors from Taiwanese patients, to elucidate the molecular pathogenesis of this tumor.

Materials and Methods

Study Subjects

Six paraffin-embedded tumor tissue samples (W7 to W12, 4 males and 2 females) from Wilms tumor patients were provided by the Department of Pediatrics of National Taiwan University Hospital. None of the patients in this study were diagnosed with Denys-Drash syndrome, Frasier syndrome or Beckwith-Wiedemann syndrome. The study procedures were approved by the Institutional Review Board of Chung Shan Medical University Hospital.

Histological Examination

The tumor tissues embedded in paraffin were sectioned at a thickness of 5 μm. Then, the sections were stained with hematoxylin and eosin and reviewed by two of the authors (T-C Hou and C-Y Kuo). Histologically, Wilms tumor is comprised of varying proportions of blastemal, stromal, and epithelial cellular components [8, 16]. Wilms tumors made up of more than two-thirds epithelial components are designated as epithelial, whereas Wilms tumors made up of more than two-thirds stromal elements are categorized as stromal [8]. If neither of these components is predominant, the tumor is designated as mixed [8].

DNA Extraction

Genomic DNA was extracted from the sections with the QIAamp Tissue Kit (Qiagen), according to the manufacturer's instructions and finally dissolved in 100 μl of TE buffer (10 mM Tris-HCl, pH 8.0, and 1 mM EDTA). DNA concentration of each sample was measured using NanoDrop UV-VIS Spectrophotometer. These DNA samples from peripheral blood lymphocytes and paraffin-embedded tumor specimens of Wilms tumors test negative for both constitutional mutations and somatic mutations in the *WT1* gene in our previous studies [12].

Array Comparative Genomic Hybridization (aCGH) Analysis

Samples were screened on 60-K oligonucleotide CGH analysis at 0.1-Mb resolution, with SurePrint G3 ISCA V2 CGH Microarray Kit (Agilent). Random primed labeling sample and reference genomic DNAs (Promega) were prepared with Genomic DNA Enzymatic Labeling Kit (Agilent). Purification was carried out according to the manufacturer's protocol. Labeled sample DNA (400 ng) was co-precipitated with an equal volume of labeled reference DNA (Promega) and 2.5 μg/μl human COT-1 DNA. The samples were hybridized to the microarray at 65 °C for 40 h. Scanning and image acquisition were carried out on Agilent Microarray Scanner D (Agilent). Data analysis was performed with Feature Extraction software v10.5 (Agilent). Copy number was determined by a conservative log2 ratio threshold. Amp refers to amplification (gain ≥0.25) and Del refers to deletion (loss ≤ −0.25). Profile deviations consisting of 10 or more neighboring oligonucleotides were considered genomic aberrations.

Results

Typing of Wilms Tumor by Pathologic Features

Microscopically, the blastemal component, the least differentiated cellular element, was predominant in W7 (hematoxylin and eosin staining, 400X in Fig. 1a). W8 showed epithelial predominance with a range of differentiation (Fig. 1b). W9 revealed mixed pattern of the three types of cellular components. However, more than two-thirds were blastemal and epithelial (Fig. 1c). The stromal component, composed of undifferentiated mesenchymal cells, was predominant in W10 and W11 (Fig. 1d and e). W12 was of mixed pattern with blastemal and epithelial cellular components (Fig. 1f).

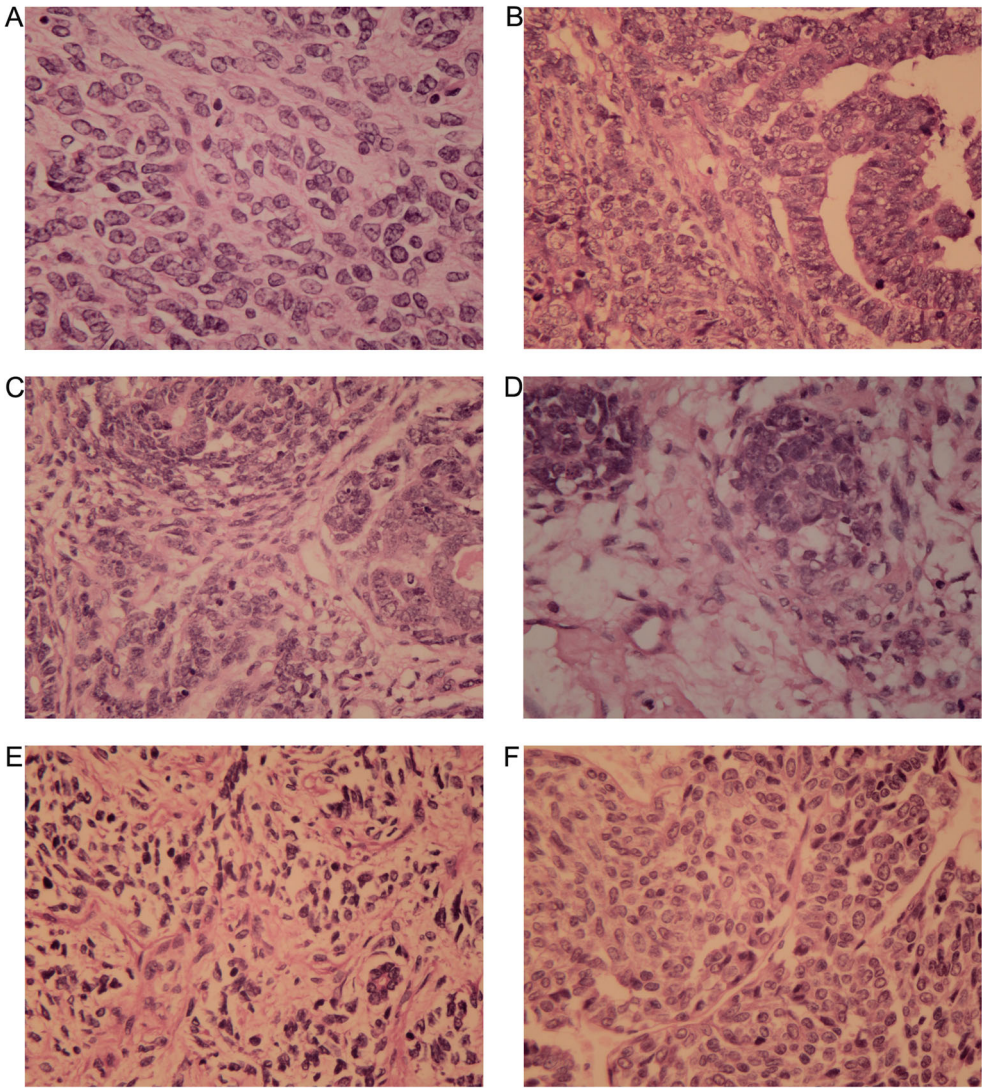

Fig. 1 Histological cross-sections after hematoxylin and eosin staining show the Wilms tumor components: blastemal, stromal, and epithelial. W7 (**a**) is blastemal. W8 (**b**) is epithelial. W9 (**c**) is mixed with stromal, blastemal, and epithelial. W10 (**d**) and W11 (**e**) are stromal. W12 (**f**) is mixed blastemal and epithelial

Array Comparative Genomic Hybridization (aCGH) Analysis

Microarray comprised of 60,000 oligonucleotide probes, with a genome-wide resolution of approximately 0.1 Mb and high sensitivity, was used in this study. Derivative log ratio spreads (DLRs) for W7, W8, and W11 were 0.179, 0.319, and 0.262 respectively. We performed analysis twice for W9 and W10 and thrice for W12 to achieve DLRs of 0.750, 0.747, and 0.434 respectively. Many chromosomal aberrations on aCGH analysis (Fig. 2) revealed that the genetics of Wilms tumors are extremely complex. Amplifications of large DNA fragments were observed, for example 1q24.2-q44 in W7 and W10, 8q12.1-q24.22 and 12q12-q24.31 in W10 and W12 (Fig. 2). There was deletion of large DNA fragment 11p15-p12 in W8. Moreover, in W12, there were deletions of large DNA fragments 16q22.1-q24.3, Xp11.1-p22.3 and Xq11.1-q27.3.

Chromosomal aberrations present in more than three Wilms tumors are shown more detail in an additional file [see Additional file 1]. The most common chromosomal aberrations were amplifications. For example, amplifications (average log2 ratio 0.935, 1.088, 0.875, 1.341, 1.242, 0.781, and 0.615, respectively) of *NDUFV1* at 11q13.2, *ZIC2* at 13q32.3, *SIX1* at 14q23.1, *NR2F2-AS1, NR2F2* and *MIR1469* at 15q26.2, *SOX9* at 17q24.3, *JAG1* and *MIR6870* at 20p12.2, and *GNAS* at 20q13.32 were observed in all six Wilms tumors (Fig. 3a, Additional file 2). In addition, amplifications (average 0.519, 1.545, and 0.695, respectively) of *SOX2-OT* and *SOX2* at 3q26.32, *GMDS* at 6p25.3, and *PLAGL1* and *HYMAI* at 6q24.2 were present in W9, W10, and W11 (Fig. 3b, Additional file 2).

Moreover, amplifications (average 0.772, 0.869, 0.633, 1.110, 0.869, and 1.190, respectively) of *SPEN, MIR5096, ZBTB17, C1orf64*, and *HSPB7* at 1p36.21-p36.1, *MYCNOS* at 2p24.3, *ZNF608* at 5q23.2, *CPA5, CPA1, TSGA14, MEST, MESTIT1*, and *MIR335* at 7q32.2, *EYA1* at 8q13.3 and

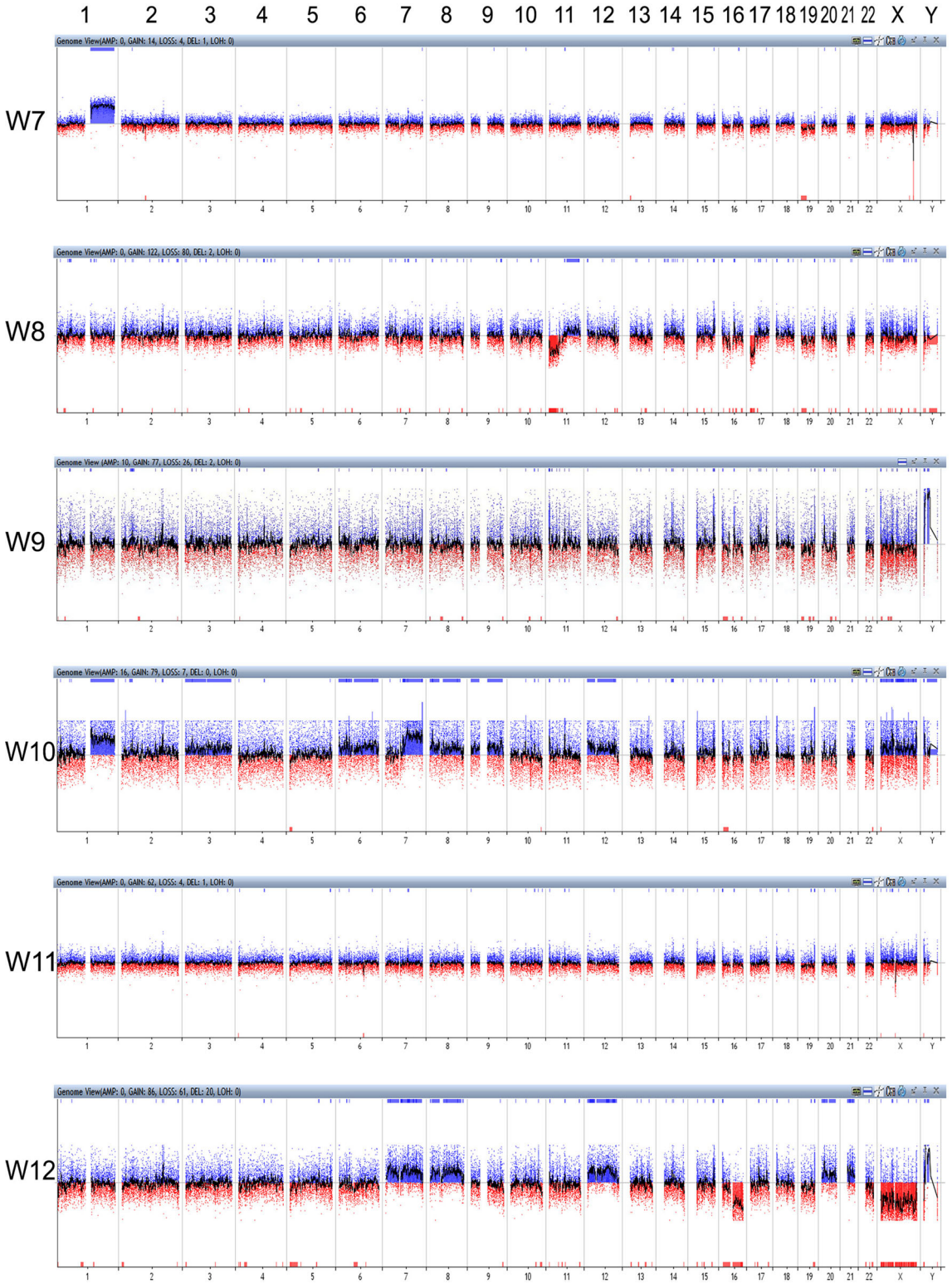

Fig. 2 Array comparative genomic hybridization analysis: Whole genomic view (Amp/Del) of comparative genomic hybridization array shows pathological genetic imbalances in many chromosomes in W7 to W12

HNF1B at 17q12 in the *FWT1* region and deletions (average −0.634, −0.449, −0.528, −0.678, −0.753, −0.679, −0.472. −0.492, and −0.609, respectively) of *MIR4417, MIR4689, NPHP4, KCNAB2,* and *CHD5* at 1p36.32-p36.31, *COL5A1* and more than 100 genes at 9q34.3, *TDRD9* and over 40 genes at 14q32.33, *CDH13, MIR3182, LOC102724163,* and *HSBP1*

A In all six Wilms tumors

Cytoband	W7	W8	W9	w10	W11	W12	Gene Names
11q13.2	0.250	0.476	1.539	1.923	0.597	0.825	NDUFV1
13q32.3	0.333	0.706	2.023	2.031	0.398	1.039	ZIC2
14q23.1	0.340	0.832	1.913	1.138	0.507	0.522	SIX1
15q26.2	0.387	1.494	2.523	1.577	0.604	1.464	NR2F2-AS1, NR2F2, MIR1469
17q24.3	0.427	0.675	2.079	2.033	0.808	1.429	SOX9
20p12.2	0.257	0.492	1.518	1.029	0.357	1.030	JAG1, MIR6870, LOC101929395
20q13.32	0.394	0.290	0.816	0.858	0.336	0.995	GNAS, LOC101927932

B In three stromal Wilms tumors

Cytoband	W9	w10	W11	Gene Names
3q26.32	0.901	0.350	0.306	SOX2-OT, SOX2
6p25.3	1.247	0.490	0.347	GMDS
6q24.2	1.905	2.275	0.456	PLAGL1, HYMAI

C In three epithelial Wilms tumors

Cytoband	W8	W9	W12	Gene Names
1p36.32 - p36.31	-0.394	-1.017	-0.490	MIR4417, MIR4689, NPHP4, KCNAB2, CHD5
9q34.3	-0.269	-0.644	-0.433	COL5A1 and more than 100 genes
14q32.33	-0.354	-0.742	-0.488	TDRD9 and over 40 genes
16q11.2 - q12.1	-0.408	-0.634	-0.990	ANKRD26P1 and 21 genes
16q23.3	-0.557	-0.476	-1.226	CDH13, MIR3182, LOC102724163, HSBP1
16q24.2 - q24.3	-0.336	-0.476	-1.226	JPH3 and more than 50 genes
19q13.33 - q13.43	-0.405	-0.547	-0.463	IZUMO2 and more than 300 genes
Xp21.1	-0.254	-0.444	-1.129	DMD and 11 genes
Xp11.4 - p11.3	-0.257	-0.296	-0.924	CASK and 5 genes
1p36.21 - p36.13	0.367	1.261	0.689	SPEN, MIR5096, ZBTB17, C1orf64, HSPB7
2p24.3	0.746	0.969	0.891	MYCNOS
5q23.2	0.65	0.77	0.48	LINC01170, ZNF608, LOC101927421
7q32.2	0.667	1.172	1.492	CPA5, CPA1, TSGA14, MEST, MESTIT1, MIR335
8q13.3	0.487	0.956	1.163	EYA1
17q12	0.924	1.450	1.197	HNF1B

D In the *WT2* region

Cytoband	W7	W8	W9	w10	W11	W12	Gene Names
11p15.5	0.000	0.000	1.770	1.863	0.643	0.486	HOTS, H19, MIR675
11p15.5	0.000	-0.379	0.896	0.876	0.000	0.486	H19, INS-IGF2, IGF2
11p15.5	0.000	-0.294	2.116	0.876	0.000	0.486	KCNQ1, KCNQ1OT1
11p15.5-p15.4	0.000	-0.294	0.896	0.876	0.000	0.486	KCNQ1, KCNQ1OT1, KCNQ1DN, CDKN1C, SLC22A18AS, SLC22A18

Fig. 3 Chromosomal aberrations on array comparative genomic hybridization (aCGH) analysis present in all six Wilms tumors (**a**), in three stromal Wilms tumors (**b**), in three epithelial Wilms tumors (**c**), and in the *WT2* region (**d**)

at 16q23.3, *ANKRD26P1* and 21 genes at 16q11.2-q12.1, *JPH3* and more than 50 genes at 16q24.2-q24.3, *IZUMO2* and more than 300 genes at 19q13.33-q13.43, *CASK, PPP1R2P9, LOC101927501, MAOA, MAOB,* and *NDP* at Xp11.4-p11.3, and *DMD* and 11 genes at Xp21.1 were identified in W8, W9, and W12 (Fig. 3c, Additional file 2).

In the *WT2* neighboring H19DMR (differentially methylated region) region at 11p15.5, amplifications (average 1.190) of *HOTS, H19,* and *MIR675* region were observed in W9 to W12 and amplifications (average 0.753) of *H19, INS-IGF2,* and *IGF2* were observed in W9, W10, and W12 (Fig. 3d, Additional file 2). Finally, amplifications (average 1.159) of *KCNQ1* and *KCNQ1OT1* neighboring KvDMR region were found in W9, W10, and W12 (Fig. 3d, Additional file 2).

Discussion

Cytogenetic abnormalities are common to Wilms tumor [16]. Kullendorff et al. demonstrated that 1q partial gains and trisomy 8 and 12 are associated with Wilms tumor [17]. Gain of 1q is associated with poor outcome [18], while 11p and 16q partial losses are associated with Wilms tumor [16, 19]. The results of this study regarding amplifications of 1q24.2-q44 in W7, 1q21.1-q44 and 7q11.23-q36.3 in W10, and 7q11.21-q36.3 in W12 are consistent with the findings of several previous studies [17, 18, 20]. Our results demonstrated partly or completely missing X chromosome in W12 (Fig. 2), suggesting that W12 is a Wilms tumor in Turner syndrome. A similar case was reported by Say et al. [21]. Genomic imbalances identified at chromosome 2p24.3 were consistent with the results of previous aCGH studies, which reveal unbalanced gain in the *MYCN* region in Wilms tumors (Additional file 1) [22, 23]. Our results pointed to the candidate genes, including *DLX1* and *DLX2* at 2q31.1, *SIX1* at 14q23.1, and *SALL1* at 16q12.1, consistent with the findings of Ruteshouser et al. which implicate 2q, 14q, and 16q in the etiology of Wilms tumor (Additional file 1) [10, 11]. Moreover, 11p15 loss of heterozygosity is uniformly an early event in Wilms tumor development [24]. Deletions of *ASCL2, C11orf21, TSPAN32, CD81, TSSC4, TRPM5, KCNQ1,* and *KCNQ1OT1* in the *WT2* region at 11p15.5 were confirmed

by the deletion of a large region of maternal 11p15.5 (2,239,763 - 42,771,741) in W8 (Fig. 2, and Additional file 1 and 2). These results were consistent with those of Al-Hussain et al. in which deletion in *WT2* is associated with epithelial or blastemal predominant Wilms tumor [8].

Wilms tumor is genetically heterogeneous. Amplification is defined as the presence of a certain number of extra gene copies, as with neuroblastoma (e.g., *MYCN*) [25]. This phenomenon can be explained by hyperdiploidy with additions of single chromosomes or portions thereof. Our findings of amplifications of *SIX1* at 14q23.1, *MYCN* at 2p24.3, and *SALL1* at 16q12.1 are consistent with the results of Gadd et al. [26]. Amplifications of *NDUFV1* at 11q13.2, *ZIC2* at 13q32.3, *SIX1* at 14q23.1, *NR2F2* and *MIR1469* at 15q26.2, *SOX9* at 17q24.3, *JAG1* and *MIR6870* at 20p12.2, and *GNAS* at 20q13.32 in all six Wilms tumors (Fig. 3a, and Additional file 1 and 2) indicated that these genes are candidate and, therefore, important to tumorigenesis. Overexpression of *SIX1* is a prognostic marker for colorectal cancer, prostate cancer, and gastric tumors [27–29]. *NR2F2* gene encodes nuclear hormone receptor (nuclear receptor subfamily 2, group F, member 2), which plays a critical role in controlling the development of a number of tissues [30, 31] and regulates metastasis of colorectal adenocarcinoma cells [32]. Our hypothesis is that amplifications of these genes may be involved in the essential events leading to tumorigenesis of Wilms tumor.

Molecular genetic classification of Wilms tumors remains to be clarified due to lack of molecular information. However, we can compare the genetic heterogeneity of inter-patient variability and histological appearances for further stratification. Histologically, W7 was classified as blastemal type, W8 as epithelial type, W10 and W11 as stromal type, and W9 and W12 as mixed pattern with varying proportions of two or three types of cellular components (Fig. 1). The mixed type may be the heterogeneous group that can be classified using these genetic results. Amplifications of *SOX2-OT* and *SOX3* at 3q26.32, *GMDS* at 6p25.3, and *PLAGL1* and *HYMAI* at 6q24.2 were observed in the three Wilms tumors of stromal type, W9, W10, and W11 (Fig. 3b, Additional file 2). The stromal type Wilms tumor may be identified using anti-SOX3 or anti-PLAGL. Amplifications of *MYCNOS* at 2p24.3, *EYA1* at 8q13.3, *HNF1B* at 17q12 were observed in the three Wilms tumors of epithelial type, W8, W9, and W12, and losses of 1p36.32 - p36.31, 9p24.3, 14q32.33, 16q 23.3, 16q11.2 - q12.1, 19q13.33 - q13.43, Xp11.4 - p11.3, and Xp21.1 were observed in the three Wilms tumors of stromal type, W9, W10, and W11 (Fig. 3c, Additional file 2). The epithelial type Wilms tumors may be a unique and isolated subgroup that can be identified with antibodies such as anti-MYCNOS, anti-EYA1, or anti-HNF-1beta (hepatocyte nuclear factor-1beta) immunohistochemistry.

Molecular analysis may inform clinical and therapeutic management of these tumors. *MIR1469* and *MIR6870* have the highest number of potential targets and may play a significant role in Wilms tumors. Up-regulated miR-1469 is associated with lymphangiogenesis in human gastric cancer [33], clear cell renal cell carcinoma [34], and chronic myeloid leukemia [35]. MiR-6870 has been detected in NUT midline carcinoma [36]. Amplifications of MIR5096 and MIR335 were observed in the three Wilms tumors of epithelial type, W8, W9, and W12 (Fig. 3b). MiR-5096 has been detected in glioma cells and elimination of miR-5096 in astrocytes has been found to decrease glioma invasion [37]. In addition, Yan et al. identified miR-335 as a prognostic signature in gastric cancer [38].

There are several limitations to this study. First, some samples were not within acceptable quality control limits. Despite this, DLR is not the only assessment of microarray probe data quality. DNA from formalin-fixed, paraffin-embedded tissues may have been highly degraded leading to increased noise in microarray data and false copy number gains/amplifications and losses. However, it is improbable for noisy data to repeatedly recur. Second, the size limit of detectable copy number abnormalities using this array was an issue. The effective resolution of the microarray comprised of 60,000 oligonucleotide probes was approximately 100 Kb. This array can potentially detect abnormalities down to ~15–20 Kb, provided there are sufficient probes in the region, but at <10 Kb it may be not reliable. Even so, there were six probes for detecting the narrow region of 589 bp of *MYCN* at 2p24.3. Third, our samples were all from Taiwanese patients. Therefore, a population-based effect, such as founder effect, could not be excluded. Additional studies based on a larger number of cases, preferably international, are necessary to confirm our conclusions regarding tumorigenesis and pathognomonic findings.

Conclusions

In summary, our results indicated that amplifications of *NDUFV1*, *ZIC2*, *SIX1*, *NR2F2, MIR1469*, *JAG1*, *MIR6870, SOX9*, and *GNAS* may be the essential events in the tumorigenesis of Wilms tumor. Stromal type Wilms tumors may be specifically associated with amplifications of five genes and epithelial type Wilms tumors may be specifically associated with amplifications of at least 10 genes. Mixed type Wilms tumors with either epithelial or stromal component can be identified using these genetic technologies, which will help to further refine the molecular classification of Wilms tumors. The epithelial components of Wilms tumors may present a unique subgroup and should be isolated from the mixed or undifferentiated type. However, larger sample size is required to provide new insight into the molecular pathogenesis of Wilms tumor. We will continue to work to clarify the role of

these chromosomal aberrations in the renal tumorigenesis of Wilms tumor.

Acknowledgements This research was supported by Research Grant CSMU-JAH-106-02 from Chung Shan Medical University-Jen-Ai Hospital. The authors would like to thank GenePhile Bioscience Laboratory of Ko's Obstetrics and Gynecology Clinic for help with acquisition of data.

Compliance with Ethical Standards

Conflict of Interest The authors declare that they have no competing interests.

Ethics Approval and Consent to Participate This study was approved by the Institutional Review Board of Chung Shan Medical University Hospital via grant reference CS2-16003.

Consent for Publication Not applicable.

References

1. Brown KW, Malik KT (2001) The molecular biology of Wilms tumour. Expert Rev Mol Med 2001:1–16
2. Pastore G, Znaor A, Spreafico F, Graf N, Pritchard-Jones K, Steliarova-Foucher E (2006) Malignant renal tumours incidence and survival in European children (1978-1997): report from the Automated Childhood Cancer Information System project. Eur J Cancer 42:2103–2114
3. Steliarova-Foucher E, Colombet M, Ries LAG, Moreno F, Dolya A, Bray F et al (2017) International incidence of childhood cancer, 2001-10: a population-based registry study. Lancet Oncol 18:719–731
4. Stiller CA, Parkin DM (1990) International variations in the incidence of childhood renal tumours. Br J Cancer 62:1026–1030
5. Hung IJ, Chang WH, Yang CP, Jaing TH, Liang DC, Lin KH et al (2004) Epidemiology, clinical features and treatment outcome of Wilms' tumor in Taiwan: a report from Taiwan Pediatric Oncology Group. J Formos Med Assoc 103:104–111
6. Coppes MJ, Egeler RM (1999) Genetics of Wilms' tumor. Semin Urol Oncol 17:2–10
7. Rahman N, Arbour L, Houlston R, Bonaiti-Pellie C, Abidi F, Tranchemontagne J et al (2000) Penetrance of mutations in the familial Wilms tumor gene FWT1. J Natl Cancer Inst 92:650–652
8. Al-Hussain T, Ali A, Akhtar M (2014) Wilms tumor: an update. Adv Anat Pathol 21:166–173
9. Menke A, McInnes L, Hastie ND, Schedl A (1998) The Wilms' tumor suppressor WT1: approaches to gene function. Kidney Int 53:1512–1518
10. Ruteshouser EC, Robinson SM, Huff V (2008) Wilms tumor genetics: mutations in WT1, WTX, and CTNNB1 account for only about one-third of tumors. Genes Chromosomes Cancer 47:461–470
11. Kaneko Y, Homma C, Maseki N, Sakurai M, Hata J (1991) Correlation of chromosome abnormalities with histological and clinical features in Wilms' and other childhood renal tumors. Cancer Res 51:5937–5942
12. Lu MY, Wang WC, Lin CW, Chang A, Lai YC (2014) Identification of a constitutional mutation in the WT1 gene in Taiwanese patients with Wilms tumor. Adv Biosci Biotechnol 5: 230–234
13. Rassekh SR, Chan S, Harvard C, Dix D, Qiao Y, Rajcan-Separovic E (2008) Screening for submicroscopic chromosomal rearrangements in Wilms tumor using whole-genome microarrays. Cancer Genet Cytogenet 182:84–94
14. Natrajan R, Little SE, Sodha N, Reis-Filho JS, Mackay A, Fenwick K et al (2007) Analysis by array CGH of genomic changes associated with the progression or relapse of Wilms' tumour. J Pathol 211: 52–59
15. Natrajan R, Williams RD, Grigoriadis A, Mackay A, Fenwick K, Ashworth A et al (2007) Delineation of a 1Mb breakpoint region at 1p13 in Wilms tumors by fine-tiling oligonucleotide array CGH. Genes Chromosomes Cancer 46:607–615
16. Md Zin R, Murch A, Charles A (2011) Pathology, genetics and cytogenetics of Wilms' tumour. Pathology 43:302–312
17. Kullendorff CM, Soller M, Wiebe T, Mertens F (2003) Cytogenetic findings and clinical course in a consecutive series of Wilms tumors. Cancer Genet Cytogenet 140:82–87
18. Hing S, Lu YJ, Summersgill B, King-Underwood L, Nicholson J, Grundy P et al (2001) Gain of 1q is associated with adverse outcome in favorable histology Wilms' tumors. Am J Pathol 158:393–398
19. Gow KW, Murphy JJ (2002) Cytogenetic and histologic findings in Wilms' tumor. J Pediatr Surg 37:823–827
20. Krepischi ACV, Maschietto M, Ferreira EN, Silva AG, Costa SS, da Cunha IW et al (2016) Genomic imbalances pinpoint potential oncogenes and tumor suppressors in Wilms tumors. Mol Cytogenet 9: 20
21. Say B, Balci S, Tuncbilek E (1971) 45,XO Turner's syndrome, Wilm's tumor and imperforate anus. Humangenetik 12:348–350
22. Schaub R, Burger A, Bausch D, Niggli FK, Schafer BW, Betts DR (2007) Array comparative genomic hybridization reveals unbalanced gain of the MYCN region in Wilms tumors. Cancer Genet Cytogenet 172:61–65
23. Williams RD, Al-Saadi R, Chagtai T, Popov S, Messahel B, Sebire N et al (2010) Subtype-specific FBXW7 mutation and MYCN copy number gain in Wilms' tumor. Clin Cancer Res 16:2036–2045
24. Cresswell GD, Apps JR, Chagtai T, Mifsud B, Bentley CC, Maschietto M et al (2016) Intra-tumor genetic heterogeneity in Wilms tumor: clonal evolution and clinical implications. EBioMedicine 9:120–129
25. Huang M, Weiss WA (2013) Neuroblastoma and MYCN. Cold Spring Harb Perspect Med 3:a014415
26. Gadd S, Huff V, Walz AL, Ooms A, Armstrong AE, Gerhard DS et al (2017) A Children's Oncology Group and TARGET initiative exploring the genetic landscape of Wilms tumor. Nat Genet 49: 1487–1494
27. Kahlert C, Lerbs T, Pecqueux M, Herpel E, Hoffmeister M, Jansen L et al (2015) Overexpression of SIX1 is an independent prognostic marker in stage I-III colorectal cancer. Int J Cancer 137:2104–2113
28. Tian T, Li A, Lu H, Luo R, Zhang M, Li Z (2015) Six1 promotes glioblastoma cell proliferation and invasion by upregulation of connective tissue growth factor. Am J Cancer Res 5:1823–1830
29. Emadi-Baygi M, Nikpour PEmadi-Andani E (2015) SIX1 overexpression in diffuse-type and grade III gastric tumors: features that are associated with poor prognosis. Adv Biomed Res 4:139
30. Lee CT, Li L, Takamoto N, Martin JF, Demayo FJ, Tsai MJ et al (2004) The nuclear orphan receptor COUP-TFII is required for limb and skeletal muscle development. Mol Cell Biol 24:10835–10843
31. Pereira FA, Qiu Y, Zhou G, Tsai MJ, Tsai SY (1999) The orphan nuclear receptor COUP-TFII is required for angiogenesis and heart development. Genes Dev 13:1037–1049

32. Bao Y, Gu D, Feng W, Sun X, Wang X, Zhang X et al (2014) COUP-TFII regulates metastasis of colorectal adenocarcinoma cells by modulating Snail1. Br J Cancer 111:933–943
33. Yang B, Jing C, Wang J, Guo X, Chen Y, Xu R et al (2014) Identification of microRNAs associated with lymphangiogenesis in human gastric cancer. Clin Transl Oncol 16:374–379
34. White NM, Khella HW, Grigull J, Adzovic S, Youssef YM, Honey RJ et al (2011) miRNA profiling in metastatic renal cell carcinoma reveals a tumour-suppressor effect for miR-215. Br J Cancer 105: 1741–1749
35. Agatheeswaran S, Pattnayak NC, Chakraborty S (2016) Identification and functional characterization of the miRNA-gene regulatory network in chronic myeloid leukemia lineage negative cells. Sci Rep 6:32493
36. Pathak E, Bhavya MD, Atri N, Mishra R (2017) Deciphering the role of microRNAs in BRD4-NUT fusion gene induced NUT midline carcinoma. Bioinformation 13:209–213
37. Hong X, Sin WC, Harris AL, Naus CC (2015) Gap junctions modulate glioma invasion by direct transfer of microRNA. Oncotarget 6:15566–15577
38. Yan Z, Xiong Y, Xu W, Gao J, Cheng Y, Wang Z et al (2012) Identification of hsa-miR-335 as a prognostic signature in gastric cancer. PLoS One 7:e40037